Cell Reports, Volume *22*

Supplemental Information

A Forward Genetic Screen Targeting the Endothelium Reveals a Regulatory Role for the Lipid Kinase Pi4ka in Myelo- and Erythropoiesis

Safiyyah Ziyad, Jesse D. Riordan, Ann M. Cavanaugh, Trent Su, Gloria E. Hernandez, Georg Hilfenhaus, Marco Morselli, Kristine Huynh, Kevin Wang, Jau-Nian Chen, Adam J. Dupuy, and M. Luisa Iruela-Arispe

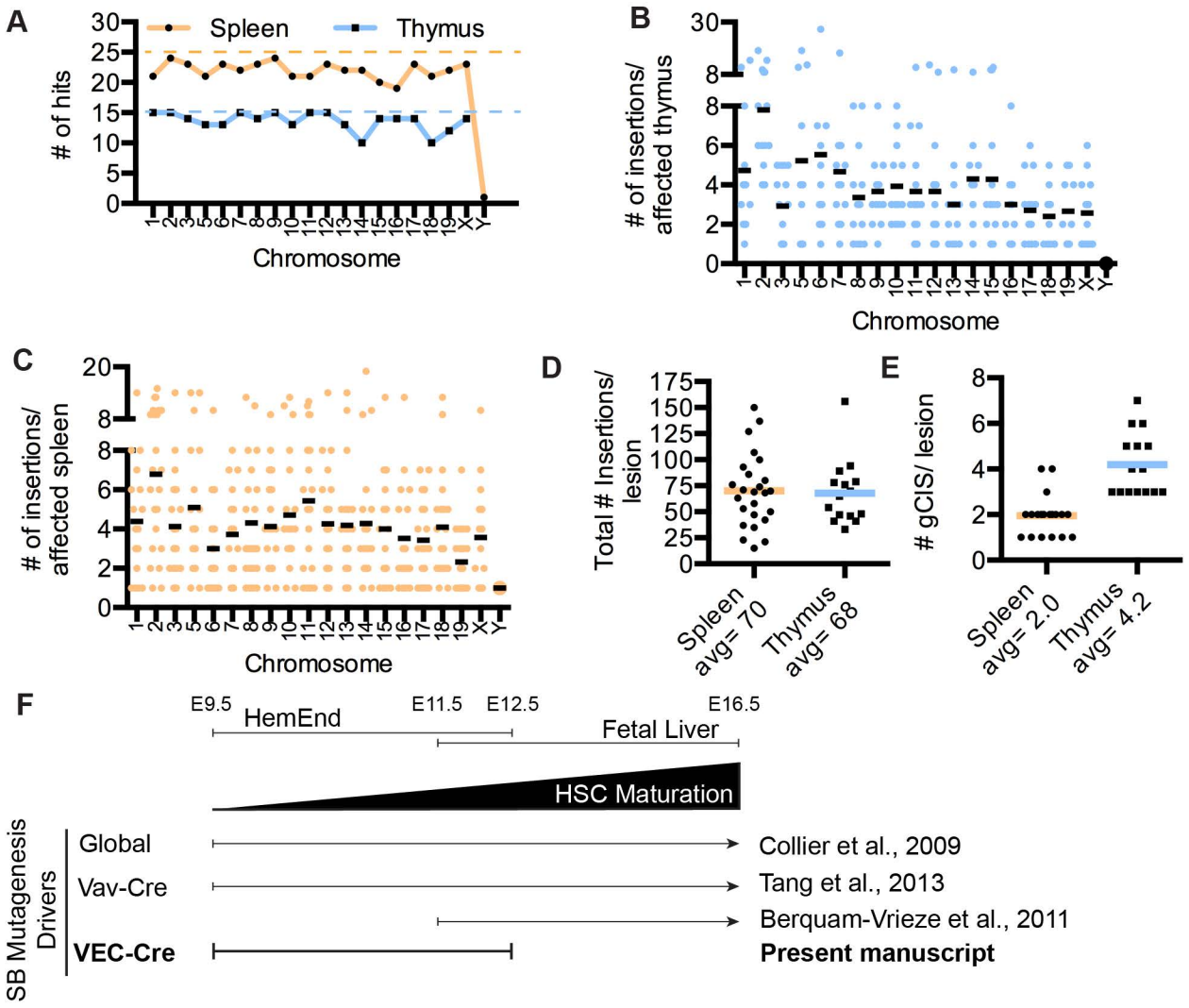

Figure S1: Transposition is unbiased, Related to Figure 2

(A) Plotting the number of hits per chromosome shows that every chromosome is hit by the transposon in both enlarged spleen and thymus tissues. Dotted lines indicate the total number of either spleen and thymus and shows that the majority of these lesions have insertions in all of the chromosomes. (B,C) The total number of insertions per spleen or thymus per chromosome shows there is little influence of chromosome size on number of insertions. Chromosome 4, the transposon donor chromosome, was removed from analysis due to preponderance of local hopping. (D) The average number of insertions per spleen is equal to that of the thymus, yet the average number of gCIS per spleen or thymus is higher in the thymus (E). (F) VEC-Cre initiates mutagenesis during a narrow time window (E9.5-12.5) This is distinct from other Cre initiated and global mutagenesis screens.

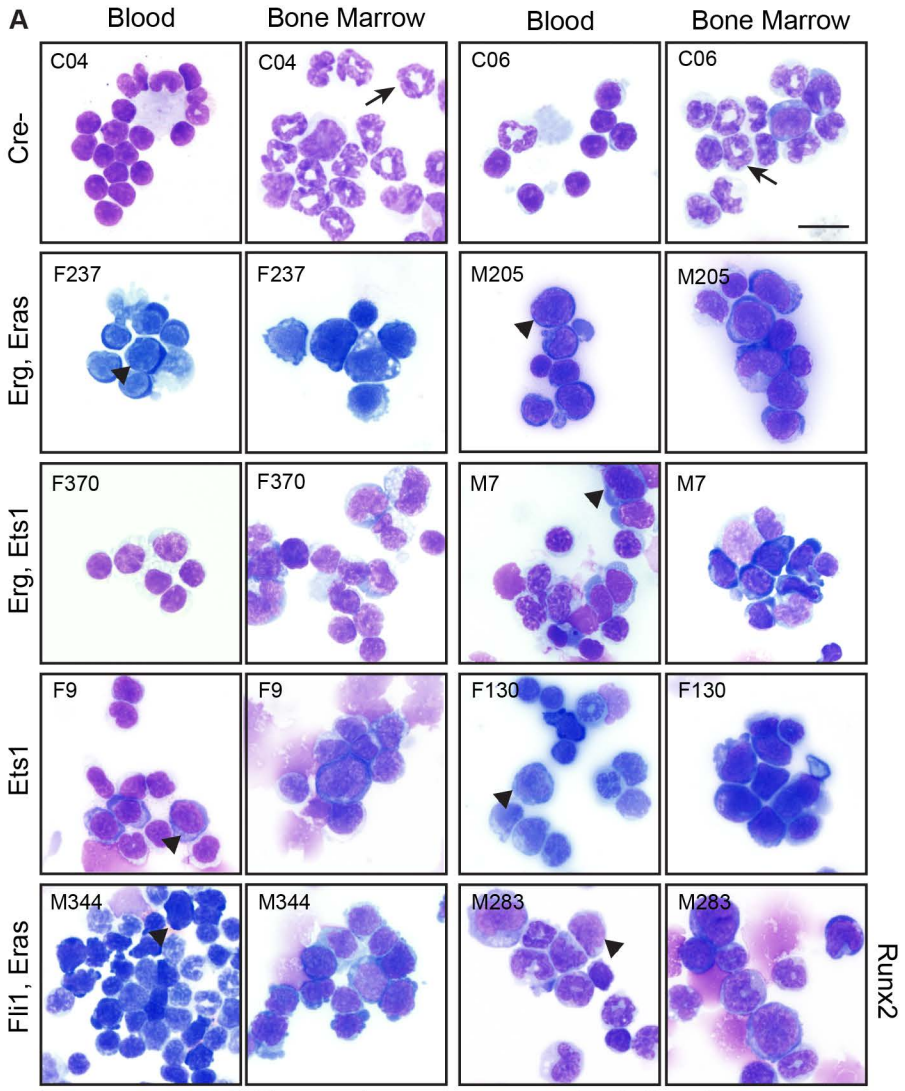

B

	M6	M332	M205	F237	F369	M344	F340	F370	M7	F9	F280	F130	M267	M278	M208	F262	M283	F270
Spleen Size	3	3	3	3	3	3	2	3	3	2	2	2	3	1	3	3	3	1
BM Blast-like	Y	Y	Y	Y	Y	Y	Y	Y	Y	Y	L	Y	Y	N/A	N/A	Y	Y	N/A
BM Neutrophils	L	L	L	L	N	N	L	N	N	N	Y	L	N	N	N/A	L	L	N/A
Blood Blast-like	Y	Y	Y	Y	Y	Y	Y	Y	Y	Y	N/A	Y	N	N	N/A	N	N	Y

Figure S2: Blast-like cells in peripheral blood and bone marrow are associated with gCIS, Related to Figure 2
(A) Mutations in certain gCIS genes were associated with a prevalence of large blast-like immature cells with high nucleus to cytoplasmic ratio in the blood and bone marrow of affected mice. A significant decrease in polymorpho-nuclear cells was observed in the bone marrow of affected animals (scale= 15μm). (arrow= polymorpho-nuclear cell, arrowhead= blast cell) (B) The majority of detected mutation patterns from Figure 2F were associated with very large spleens (3> 800mg, 800>2>500mg, 1<500mg), blast-like cells in the blood, and reduced polymorpho-nuclear cells in the bone marrow of affected animals (each column). M=male, F= female; numbers indicate individual ID number for each mouse.

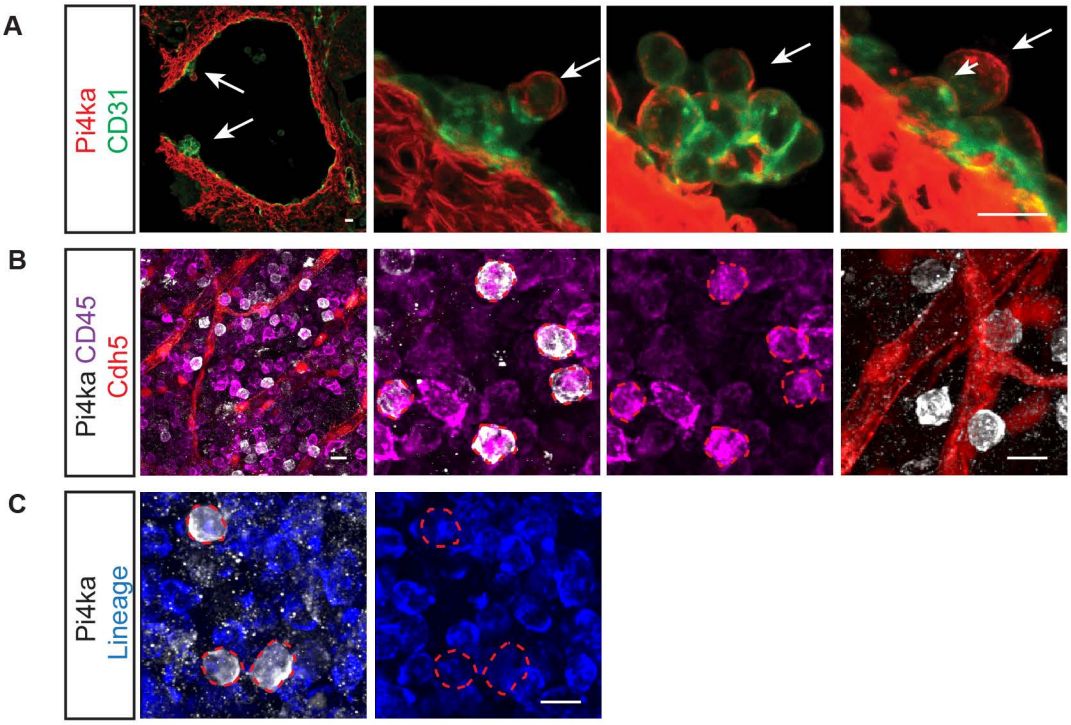

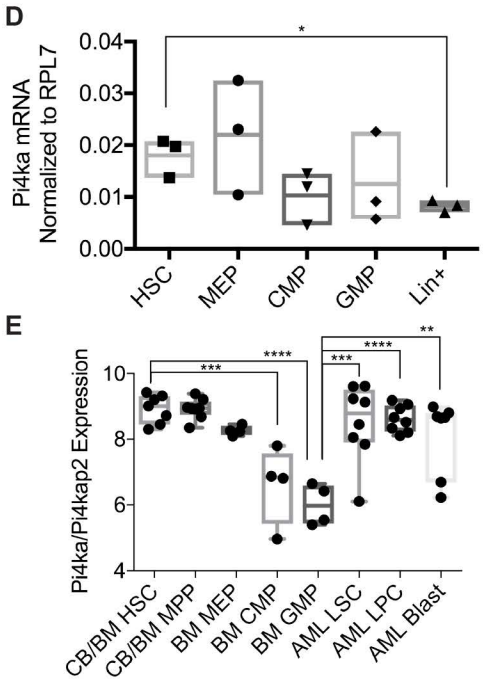

Figure S3: Pi4ka expression in HSPC budding from HemEnd and in adult lineage negative bone marrow cells, Related to Figure 4

(A) Pi4ka (red) was observed in the subaortic mesenchyme, but was also found in the membrane of the budding HSPC (CD31 positive, green) from hemogenic E9.5 aorta. (B) Pi4ka (white), CD45 (magenta), and Cdh5-Tomato vasculature (red) immunofluorescence of adult mouse bone marrow. (C) Immunofluorescence of Cdh5-Tomato adult mouse bone marrow with Pi4ka (white) and lineage cocktail (blue). (A-C, scale = 10μm) (D) Expression of Pi4ka was higher in HSC (Lin-cKit+Sca1+) and myeloid/erythroid populations of mouse adult marrow when compared to Lin+ differentiated hematopoietic cells. (E) Pi4ka/Pi4kap2 mRNA expression is higher in HSC and myeloid/erythroid lineage human populations in human bone marrow as well as in AML (BloodChIP) Graphs represent mean ± SEM comparisons done by t-test (D) or ANOVA (E). Individual samples are indicated by filled dots.

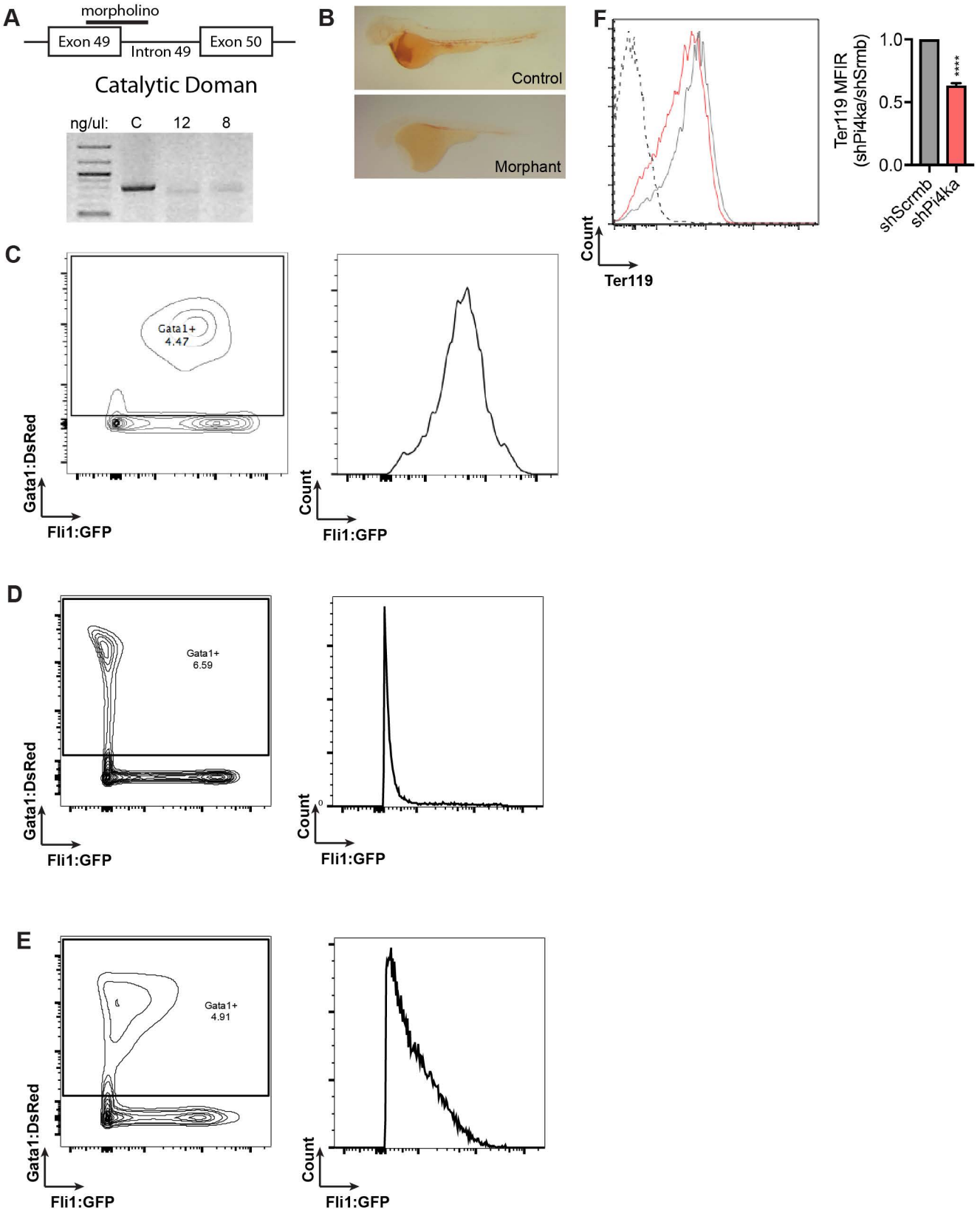

Figure S4: Loss of Pi4ka decreases erythroid differentiation in vivo and in vitro, Related to Figure 5
(A) Morpholino targeted splicing in the catalytic domain. PCR to assess splicing efficiency. (B) O-dianisidine marking hemoglobin in control and morphant fish. (C) 24 hpf control injected embryos were subjected to flow cytometry and Gata1:DsRED was plotted against Fli1:GFP (left). Histogram of Gata1:DsRED+ cells as a subpopulation of Fli1:GFP cell population. (D,E) Identical gating performed on 48 hour control (top) and morphant embryos (bottom). (F) G1E-ER4 cell differentiation in the presence of 4-hydroxytamoxifen (solid line) or ethanol control (dashed line). Cells were either pre-treated with non-targeted shRNA (grey) or Pi4ka targeted shRNA (red). Median fluorescence intensity (MFIR) was calculated as a ratio of MFI relative to shScrmb control. Statistical t-test comparing 3 independent experiments. (* $p \leq 0.05$, ** $p \leq 0.01$ ***, $p \leq 0.001$, ****, $p \leq 0.0001$)

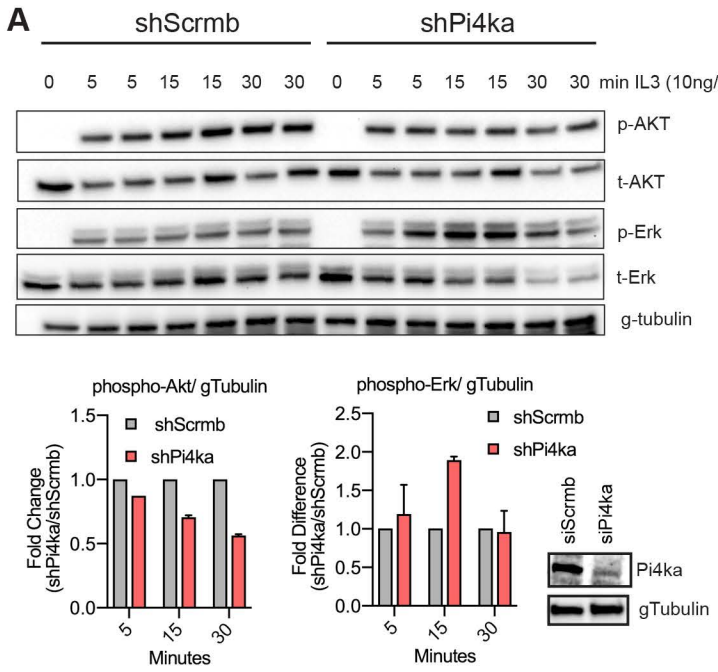

Figure S5. Loss of Pi4ka in vitro blunts Akt signaling and enhances ERK signaling, Related to Figure 6
(A) Western blot assessing AKT and ERK after IL3 stimulation of 32D cells treated with shScrmb or shPi4ka. Cells were treated with 10ng/ml IL3 for 0,5,15, and 30 minutes. Quantification of fold change of shPi4ka treated cells of shScrmb treated cells (bottom). Representative image of Pi4ka knockdown by Western.

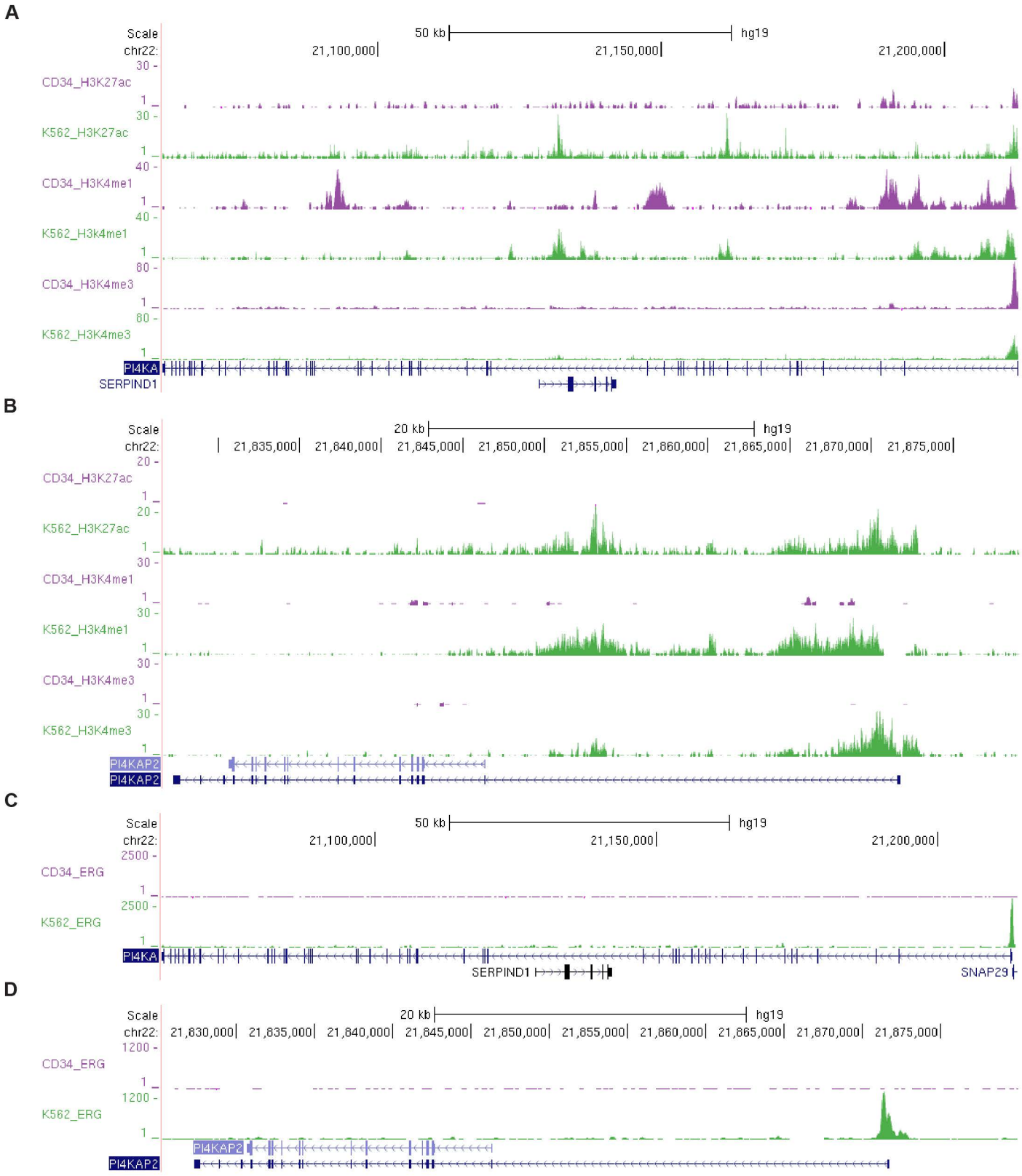

Figure S6. PI4KA and PI4KAP2 promoter transcriptional activation marks and ERG transcription factor binding, Related to Figure 7

(A) UCSC genome browser visualization of transcriptional activation acetylation and methylation marks for the PI4KA gene in human CD34+ HSPC and the human erythroleukemia cell line K562. (B) Transcriptional activaion marks for the PI4KAP2 gene in CD34+ HSPC and eythroleukemia K562 cells. (C) ERG transcription factor binding at the PI4KA promoter in CD34+ HSPC and K562 cells. (D) ERG transcription factor binding at the Pi4kap2 promoter in CD34+ HSPC and K562 cells. (BloodChIP database)

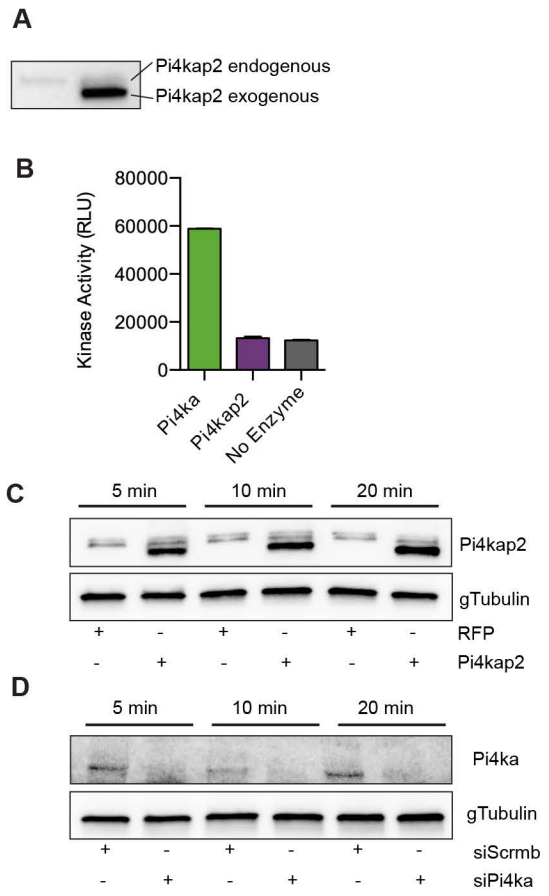

Figure S7. The human Pi4kap2 gene yields protein product, Related to Figure 7
(A) PI4KAP2 construct overexpressed in HEK293 cells. (B) Lipid kinase activity of PI4KA and PI4KAP2. (C) Confirmation of PI4KAP2 and control vector overexpression in HEK293 cells for antibody microarray experiments (D) PI4KA knockdown confirmation in HEK293 cells for antibody micro-array experiments.

Table S1. gCIS captured by VEC-Cre initiated mutagenesis compared to later developmental Cre recombinases, Related to Figure 2

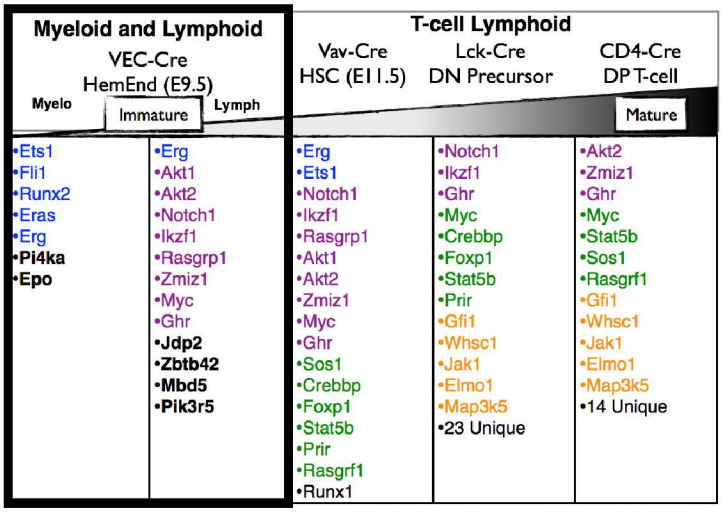

Figure S1: Transposition is unbiased, Related to Figure 2
(A) Plotting the number of hits per chromosome shows that every chromosome is hit by the transposon in both enlarged spleen and thymus tissues. Dotted lines indicate the total number of either spleen and thymus and shows that the majority of these lesions have insertions in all of the chromosomes. (B,C) The total number of insertions per spleen or thymus per chromosome shows there is little influence of chromosome size on number of insertions. Chromosome 4, the transposon donor chromosome, was removed from analysis due to preponderance of local hopping. (D) The average number of insertions per spleen is equal to that of the thymus, yet the average number of gCIS per spleen or thymus is higher in the thymus (E). (F) VEC-Cre initiates mutagenesis during a narrow time window (E9.5-12.5). This is distinct from other Cre initiated and global mutagenesis screens.

Figure S2: Blast-like cells in peripheral blood and bone marrow are associated with gCIS, Related to Figure 2
(A) Mutations in certain gCIS genes were associated with a prevalence of large blast-like immature cells with high nucleus to cytoplasmic ratio in the blood and bone marrow of affected mice. A significant decrease in polymorpho-nuclear cells was observed in the bone marrow of affected animals (scale= 15μm). (arrow= polymorpho-nuclear cell, arrowhead= blast cell) (B) The majority of detected mutation patterns from Figure 2F were associated with very large spleens (3> 800mg, 800>2>500mg, 1<500mg), blast-like cells in the blood, and reduced polymorpho-nuclear cells in the bone marrow of affected animals (each column). M=male, F= female; numbers indicate individual ID number for each mouse.

Figure S3: Pi4ka expression in HSPC budding from HemEnd and in adult lineage negative bone marrow cells, Related to Figure 4.
(A) Pi4ka (red) was observed in the subaortic mesenchyme, but was also found in the membrane of the budding HSPC (CD31 positive, green) from hemogenic E9.5 aorta. (B) Pi4ka (white), CD45 (magenta), and Cdh5-Tomato vasculature (red) immunofluorescence of adult mouse bone marrow. (C) Immunofluorescence of Cdh5-Tomato adult mouse bone marrow with Pi4ka (white) and cKit (blue). (A-C, scale = 10μm) (D) Expression of Pi4ka was higher in HSC (Lin-cKit+Sca1+) and myeloid/erythroid populations of mouse adult marrow when compared to Lin+ differentiated hematopoietic cells. (E) Pi4ka/Pi4kap2 mRNA expression is higher in HSC and myeloid/erythroid lineage human populations in human bone marrow as well as in AML (BloodChIP) Graphs represent mean ± SEM comparisons done by t-test (D) or ANOVA (E). Individual samples are indicated by filled dots.

Figure S4: Loss of Pi4ka decreases erythroid differentiation in vivo and in vitro, Related to Figure 5
(A) Morpholino targeted splicing in the catalytic domain. PCR to assess splicing efficiency. (B) O-dianisidine marking hemoglobin in control and morphant fish. (C) 24 hpf control injected embryos were subjected to flow cytometry and Gata1:DsRED was plotted against Fli1:GFP (left). Histogram of Gata1:DsRED+ cells as a subpopulation of Fli1:GFP cell population. (D,E) Identical gating performed on 48 hour control (top) and morphant embryos (bottom). (F) G1E-ER4 cell differentiation in the presence of 4-hydroxytamoxifen (solid line) or ethanol control (dashed line). Cells were either pre-treated with non-targeted shRNA (grey) or Pi4ka targeted shRNA (red). Median fluorescence intensity (MFIR) was calculated as a ratio of MFI relative to shScrmb control. Statistical t-test comparing 3 independent experiments. (* $p \leq 0.05$, ** $p \leq 0.01$ ***, $p \leq 0.001$, ****, $p \leq 0.0001$)

Figure S5. Loss of Pi4ka in vitro blunts Akt signaling and enhances ERK signaling, Related to Figure 6

(A) Western blot assessing AKT and ERK after IL3 stimulation of 32D cells treated with shScrmb or shPi4ka. Cells were treated with 10ng/ml IL3 for 0,5,15, and 30 minutes. Quantification of fold change of shPi4ka treated cells of shScrmb treated cells (bottom). Representative image of Pi4ka knockdown by Western.

Figure S6. PI4KA and PI4KAP2 promoter transcriptional activation marks and ERG transcription factor binding, Related to Figure 7

(A) UCSC genome browser visualization of transcriptional activation acetylation and methylation marks for the PI4KA gene in human CD34+ HSPC and the human erythroleukemia cell line K562. (B) Transcriptional activaion marks for the PI4KAP2 gene in CD34+ HSPC and eythroleukemia K562 cells. (C) ERG transcription factor binding at the PI4KA promoter in CD34+ HSPC and K562 cells. (D) ERG transcription factor binding at the Pi4kap2 promoter in CD34+ HSPC and K562 cells. (BloodChIP database)

Figure S7. The human Pi4kap2 gene yields protein product, Related to Figure 7

(A) PI4KAP2 construct overexpressed in HEK293 cells. (B) Lipid kinase activity of PI4KA and PI4KAP2. (C) Confirmation of PI4KAP2 and control vector overexpression in HEK293 cells for antibody microarray experiments (D) PI4KA knockdown confirmation in HEK293 cells for antibody micro-array experiments.

Supplementary Experimental Procedures

Lipid Kinase Assay

The Pi4kap2-HA protein was purified from HEK293 cells two days after transient transfection. Cells were lysed with mRIPA buffer and the tagged protein was immuno-precipitated using Pierce anti-HA agarose beads (26181 Thermo Fischer Scientific) in the presence of protease inhibitors overnight. Beads were pelleted, washed with kinase buffer and protein was eluted in kinase buffer supplemented with 1mg/ml HA peptide at RT for 15min. The *in vitro* lipid kinase assay was assembled in a white plate and kinase activity was measured as per the ADP Glo Lipid Kinase Assay Protocol (V6930 Promega). Human Pi4ka (PV5869 Thermo Fisher Scientific) or purified human Pi4kap2-HA was combined with PI:3PS lipid substrate in the presence of ATP for 1 hour. Luminescence was measured using a BMG Labtech Omega plate reader.

Immunofluorescence

For embryos, antibodies against CD31 and Pi4ka were used. Pi4ka staining was followed with biotinylated secondary and amplification was performed by Alexafluor 568 tyramide (Life Technologies). CD31 antibody was followed by Alexafluor-488 conjugated secondary. For adult bone marrow (BM), flushed strands were fixed with PFA, blocked and permeabilized. BM was stained with antibodies against Pi4ka, lineage cocktail, CD45, and fluorescent secondaries (see below). A Zeiss confocal microscope was used to image fluorescence along with Zen acquisition software (Zeiss).

G1E-ER4 differentiation assay

G1E-ER4 cells were pre-treated with non-targeted shRNA or Pi4ka targeted shRNA then FACS sorted based on GFP expression to purify knockdown cell population. Transduced G1E-ER4

cells were then cultured with 0.5U/ml 4-hydroxytamoxifen or ethanol for 48 hours. Differentiation was assessed using anti-Ter119 via flow cytometry.

Antibodies

Primary IHC/IF	**Vendor**	**Catalog #**
Pi4ka	Cell Signaling	4902
CD31	Dianova	DIA-310
Pi4ka	Proteintech	12411-1-AP
V450 lineage cocktail	BD Biosciences	561301
CD45	BD Biosciences	550539
Secondary IF	**Vendor**	**Catalog #**
anti-rat AF-488	LifeTechnologies	A21208
anti-rabbit AF-647	LifeTechnologies	A31573
Primary Western Blot		
phospho- p44/42 MAPK Erk1/2 Thr202/Tyr204	Cell Signaling	9101
total p44/42 MAPK Erk1/2	Cell Signaling	4695
phospho-Akt Ser473	Cell Signaling	9271
total Akt	Cell Signaling	9272
Pi4ka	Proteintech	12411-1-AP
Pi4kap2	Proteintech	16422-1-AP
phospho-S6 Ribosomal Protein Ser240/244	Proteintech	D68F8
beta-Actin	Sigma	
gamma tubulin	Abcam	ab11321

Primers

Morpholino	**Sequence**	**Citation**
pi4kaa splice-inhibitory	5'-AATGTGTGTAACCTTCTGGAAAGCC-3'	(H. Ma et al., 2009)
p53	5' - GCGCCATTGCTTTGCAAGAATTG - 3'	(Langheinrich et al., 2002)
Splicing Efficiency	**Sequence**	**Citation**
zebrafish *pi4kaa* Fwd	5'-GATGGCTCAAAGGGTCTGCTGGCAG-3'	(H. Ma et al., 2009)
zebrafish *pi4kaa* Rev	5'-GTCTCAGTATGGGATTTGGTTCTGG-3'	(H. Ma et al., 2009)
qPCR Primers	**Sequence**	**Citation**
zebrafish *gata1* Fwd	5'-TGAATGTGTGAATTGTGGTG-3'	(Bertrand et al., 2008)
zebrafish *gata1* Rev	5'-ATTGCGTCTCCATAGTGTTG-3'	(Bertrand et al., 2008)
zebrafish PU.1 Fwd	5'-AGAGAGGGTAACCTGGACTG-3'	(Bertrand et al., 2008)
zebrafish PU.1 Rev	5'-AAGTCCACTGGATGAATGTG-3'	(Bertrand et al., 2008)
zebrafish lmo2 Fwd	5'-AAATGAGGAGCCGGTGGAT-3'	(Bertrand et al., 2008)
zebrafish lmo2 Rev	5'-GCTCGATGGCCTTCAGAAA-3'	(Bertrand et al., 2008)
zebrafish scl alpha Fwd	5'-CTGAAATCCGAGCAATTTCC-3'	(Ren et al., 2010)
zebrafish scl alpha Rev	5'-GTTTCCTTGGCAACACCATT-3'	(Ren et al., 2010)
zebrafish mpx Fwd	5'-TGATGTTTGGTTAGGAGGTG-3'	(Bertrand et al., 2008)
zebrafish mpx Rev	5'-GAGCTGTTTTCTGTTTGGTG-3'	(Bertrand et al., 2008)
zebrafish l-plastin Fwd	5'-TGTCTGTGCCCGACACCAT-3'	(Oehlers et al., 2011)
zebrafish l-plastin Rev	5'-GGCGGAGGCAGAGTTCAG-3'	(Oehlers et al., 2011)
zebrafish b-globin e1a/b/c Fwd	5'-CTTGACCATCGTTGTTG-3'	(Ganis et al., 2012)
zebrafish b-globin e1a/b/c Rev	5'-GATGAATTTCTGGAAAGC-3'	(Ganis et al., 2012)
mouse *Pi4ka* Fwd	5'- TTCATGGAGATGTGTGTCCGAGGT-3'	
mouse *Pi4ka* primer Rev	5'- AGGCCTGTGTCCAACATGAGTGTA-3'	
mouse *Rpl7* Fwd	5'- AAGCGGATTGCCTTGACAGA-3'	
mouse *Rpl7* Rev	5'- TTCCTTGAAGCGTTTCCCGA- 3'	
human *PI4KAP1/2* specific Fwd	5'-CAACCATCCGCAATGTGCTTC-3'	
human PI4KAP1/2 specific Rev	5'-GTCAGCTGGGGGAACAAGCT-3'	
human *PI4KA* specific Fwd	5'-GCCTGGAGCATCTCTCCCTA-3'	
human *PI4KA* specific Rev	5'-AGGCACATCACTAACGGCTC-3'	
Molecular Cloning Primers	**Sequence**	
PstI PI4KAP2 Fwd	5'- CTGCAGGTTGGCATGCACCCCCAG-3'	
AgeI PI4KAP2 Rev	5'-ACCGGTTCAGGCGTAGTCAGGAACATCG TAAGGATAGTAGGGGATGTCATTCTGATAG-3'	

MNDU3GFP_Fwd_SphI	5'-GCATGCCAGGGACAGCAGAGATCCAG-3'	
MNDU3GFP_Rev2_MluL	5'-ACGCGTGGTACCGTCGACTGCAG-3'	

Supplemental References

Bertrand, J.Y., Kim, A.D., Teng, S., Traver, D., 2008. CD41+ cmyb+ precursors colonize the zebrafish pronephros by a novel migration route to initiate adult hematopoiesis. Development 135, 1853–1862. doi:10.1242/dev.015297

Ganis, J.J., Hsia, N., Trompouki, E., Jong, J.L.O. de, Dibiase, A., Lambert, J.S., Jia, Z., Sabo, P.J., Weaver, M., Sandstrom, R., Stamatoyannopoulos, J.A., Zhou, Y., Zon, L.I., 2012. Zebrafish globin switching occurs in two developmental stages and is controlled by the LCR. Dev Biol 366, 185–194. doi:10.1016/j.ydbio.2012.03.021

Langheinrich, U., Hennen, E., Stott, G., Vacun, G., 2002. Zebrafish as a model organism for the identification and characterization of drugs and genes affecting p53 signaling. Curr Biol 12, 2023–2028.

Ma, H., Blake, T., Chitnis, A., Liu, P., Balla, T., 2009. Crucial role of phosphatidylinositol 4-kinase IIIalpha in development of zebrafish pectoral fin is linked to phosphoinositide 3-kinase and FGF signaling. J Cell Sci 122, 4303–4310. doi:10.1242/jcs.057646

Oehlers, S.H., Flores, M.V., Hall, C.J., Swift, S., Crosier, K.E., Crosier, P.S., 2011. The inflammatory bowel disease (IBD) susceptibility genes NOD1 and NOD2 have conserved anti-bacterial roles in zebrafish. Disease Models & Mechanisms 4, 832–841. doi:10.1242/dmm.006122

Ren, X., Gomez, G.A., Zhang, B., Lin, S., 2010. Scl isoforms act downstream of etsrp to specify angioblasts and definitive hematopoietic stem cells. Blood 115, 5338–5346. doi:10.1182/blood-2009-09-244640